SPADES APPLICATION DEVELOPMENT AND PRODUCTION FORECAST BASED ON DRAINAGE VOLUME FORMULATION

A Thesis

by

ANKIT BANSAL

Submitted to the Office of Graduate and Professional Studies of
Texas A&M University
in partial fulfillment of the requirements for the degree of

MASTER OF SCIENCE

Chair of Committee,	Michael J. King
Committee Members,	Art Donovan
	John Lee
Head of Department,	Jeff Spath

August 2020

Major Subject: Petroleum Engineering

ABSTRACT

Unconventional resources have recently gained significant momentum in the industry while the scientific understanding of these resources are primarily under research. Due to the large scale of activities with hundreds of wells drilled, significant optimization to improve efficiency is carried out by data driven technologies. These resources require detailed understanding like hydraulic fracturing, horizontal drilling to understand the productivity of a well.

To understand the complex fracture geometry, we develop the asymptotic solution of the diffusivity equation. We implement the time evolution of the $w(\tau)$ function, which characterizes the flow geometry of the transient drainage volume. It allows us to identify linear flow, onset of fracture interference, matrix permeability, fracture half length, fracture surface area and the volume of SRV. A software (SPADES) was developed on a Python-Excel platform. The application uses Python based scientific libraries and an Excel bases user-interface to calculate the diagnostic plots. The application implements Outlier and Noise removal algorithms, and automates the tuning parameters.

Production forecast based on the transient solution of the drainage volume formulation and is an analytical solution based on the reservoir properties. Reservoir properties like matrix permeability, fracture half length, hydraulic diffusivity is determined from the $w(\tau)$ function. The forecast is based on an elliptical drainage model where the $w(\tau)$ function extrapolated up to the expected reservoir volume. This technique may be used to forecast

the pressure–production performance, EUR, UR and productivity index. We demonstrate the technique on a finite element simulator and an Eagle Ford well using a production rate history match and flowing material balance. Further, sensitivity analysis is performed to understand the parameters affecting this analytic technique.

The SPADES application may be used by exploration & production companies to understand the behaviour of their wells and select refracturing candidates, while the production forecast can be a reliable source of forecast for reserve booking and economic analysis.

DEDICATION

This work is dedicated to my family and my wonderful fiancée, Aprajita, who supported me through my graduate school.

I also dedicate this study to every individual who pursues research with a passion to make this world a better place.

ACKNOWLEDGEMENTS

I would like to thank my committee chair, Dr. M. J. King, and my committee members, Dr. A. Donovan, and Dr. J. Lee, for their guidance and support throughout the course of this research.

I also thank my friends, colleagues, the department faculty, and staff for making my time at Texas A&M University a wonderful experience. I am also thankful to the MCERI group for providing the platform and exposure to pursue world class research. I am also thankful to Oil India Limited for providing a two year study leave to pursue this degree.

Finally, I thank my family, my mother, father, sister and fiancée for their encouragement and support to pursue my passion for research.

CONTRIBUTORS AND FUNDING SOURCES

Contributors

This work was supervised by a thesis committee consisting of Dr Michael J King and Dr John Lee of the Harold Vance Department of Petroleum Engineering and Dr Art Donovan of the Department of Geology and Geophysics.

The data analyzed for Chapter 3 was provided by Marathon Oil EF LLC. The analyses depicted in Chapter 2 and Chapter 3 was conducted in part by members of the MCERI group, Dr Zhenzhen Wang, Dr Xu Xue and Mr Andrew Malone, of the Harold Vance Department of Petroleum Engineering.

All other work conducted for the thesis was completed by the student independently.

Funding Sources

Graduate study was supported by a fellowship from Texas A&M University and by the financial support of the member companies of the Model Calibration and Efficient Reservoir Imaging (MCERI) consortium.

TABLE OF CONTENTS

Page

LIST OF FIGURES

Page

LIST OF TABLES

Page

NOMENCLATURE

A_f	total fracture surface area
B	formation volume factor (rb/stb)
C_i	convolution coefficients for Savittzky Golay algorithm
c_t	total compressibility (1/psi)
f(t)	input signal for Savitzky Golay algorithm window size selection
h	formation thickness
J	well productivity (stb/psi/day)
JBDF	well productivity under boundary dominated flow (stb/psi/day)
JPSS	well productivity under pseudo steady state (stb/psi/day)
k	permeability (mD)
k_m	matrix permeability (mD)
K	number of model parameters
l_w	length of well lateral (ft)
n_{SG}	order of Savitzky Golay filter
n_f	number of hydraulic fractures
N_k	neighboring point at distance atleast k or k

N_{opt}	Optimum window length for Savitzky Golay algorithm
p	pressure (psi)
p_i	initial reservoir pressure (psi)
p_{wf}	bottom hole flowing pressure (psi)
PV	reservoir pore volume (ft^3)
q	flux (stb/day)
q_w	well flux at sand face (stb/day)
Q	cumulative production (stb)
Q_w	cumulative well flux at sand face (stb/day)
t	time (hr)
t_e	material balance time (hr)
$V(t)$	time dependent volume
$V_p(\tau)$	pore volume (ft^3)
$V_d(t)$	drainage volume (ft^3)
V_{res}	reservoir volume (ft^3)
$w(\tau)$	derivative of pore volume with respect to τ ($ft^3/hr^{1/2}$)
$\vec{x}$	cartesian spatial coordinate vector
x_f	fracture half length

x_s	well spacing
y	input noisy signal for Savitzky Golay algorithm
Y	smooth data points obtained from Savitzky Golay algorithm
α	diffusivity (ft^2/hr)
α_k	coefficient of the k^{th} basis function
ϕ	porosity (vol/vol)
$\phi_k(\tau)$	the kth basis function
σ	standard deviation
$\widehat{\sigma^2}$	residual Sum of Squares
ξ	boltzmann variable (dimensionless)
λ	weight of the roughness penalty term
τ	diffusive time of flight ($hr^{1/2}$)
τ_{elf}	end of linear flow in terms of diffusive time of flight ($hr^{1/2}$)
τ_{ifi}	initiation of fracture interference in terms of diffusive time of flight ($hr^{1/2}$)
τ_{lf}	linear flow in terms of diffusive time of flight ($hr^{1/2}$)
τ_e	diffusive time of flight at reservoir boundary ($hr^{1/2}$)
μ	fluid viscosity (cp)

1-D	One Dimensional
2-D	Two Dimensional
3-D	Three Dimensional
AIC	Akaike Information Criterion
API	Application Program Interface
BDF	Boundary Dominated Flow
BHP	Bottom Hole Pressure
BIC	Bayesian Information Criterion
DTOF	Diffusive Time of Flight
EUR	Estimated Ultimate Recovery
IRR	Instantaneous Recovery Ratio
lrd	Local Reachability Distance
LOF	Local Outlier Factor
RTA	Rate Transient Analysis
RNP	Rate Normalized Pressure
RSS	Residual Sum of Squares
PI	Productivity Index
PTA	Pressure Transient Analysis

UI	User Interface
UR	Ultimate Recovery
VBA	Visual Basic for Applications

CHAPTER I

INTRODUCTION

Unconventional tight/shale reservoirs have become an important component of the global energy supply. They can be described as hydrocarbon accumulations which are difficult to be characterized and produced by conventional exploration and production technologies (Ilk, Jenkins, & Blasingame, 2011). Production from unconventional oil reservoirs has become a major source of the United States crude oil supply and accounts for 63% of US crude oil production (EIA, 2020). The tight/shale reservoirs are characterized by very low permeability which require horizontal wells with multistage hydraulic fractures for stimulation. The wide application of hydraulic fracturing techniques lead to complex fracture geometries with large effective areas (Wang, Malone, & King, 2019). These reservoirs produce with depletion drive as the primary recovery mechanism. They usually have a very long transient period that is orders of magnitude longer than conventional reservoirs. and have a relatively short or even no production under boundary dominated flow before well abandonment. In these reservoirs, understanding the pressure front propagation is very important to characterize the reservoir behavior in terms of drainage volume, limit of detectability, radius of investigation, flow regime identification, and, estimate matrix permeability, fracture area and fracture half-length.

The highly volatile oil prices place considerable strain on the industry, increasing the importance of advancing technology that can help optimize field development plans by reducing costs and minimizing risks.

Numerical and analytical techniques are used to characterize the fracture behavior and understand the well performance. Decline curve analysis are empirical techniques generally used for production forecasting and reserve booking (Arps, 1945; Fetkovich, 1980; W. J. Lee & Sidle, 2010). Rate/Pressure transient based analytic formulation provides a description of the reservoir behavior by making simplifying assumptions about the fracture characteristic and reservoir heterogeneity (Song & Ehlig-Economides, 2011).

In this study, we develop an application named SPADES that implements a technique to characterize the drainage volume based on the asymptotic solution technique for the diffusivity equation. This application is built on an Excel-Python platform that provides a user-friendly interface for an engineer. The application is used to calculate the $w(\tau)$, IRR, drainage volume and various fracture/well completion based cross plots that help in selection of refracturing candidates.

Further, the technique is extended to production forecasts and can be used for determining the Ultimate Recovery, Estimated Ultimate Recovery and Well productivity. We validate our approach with results from a finite element simulator and also with a field case from Eagle Ford. Our study demonstrates that this approach is a reliable method for production forecasting and is based on the production data while it also provides a physics-based solution unlike other empirical solutions.

This section is divided into two parts, first to explain the theory and development of the diffusive time of flight, $w(\tau)$, drainage volume concepts and the second part emphasizes of the development of various production forecasting models for unconventional reservoirs.

Data Driven Model: Asymptotic Solution of the Diffusivity Equation

Pressure transient analysis and Rate transient analysis provide an analytical solution of simplified reservoir models and well configurations (Bourdet, 2002; Horne, 1995; J. Lee, 1982; Thambynayagam, 2011). These models can be calibrated/modified based on field responses to provide significant summaries of into the reservoir and well characteristics. These methods are ideal for generating quick yet detailed analysis of the well completion strategies for a field. Numerical simulation can generate models with large degrees of freedom that can model stress-strain behavior, fracture complexity, adsorption effects, multi-phase fluid interactions and well completion characteristics. These models require variety of input data that may be expensive to acquire and may also have uncertainties associated with them. This leads to non-unique solutions of the history match and can make it difficult to gain simple insights that an analytical model may provide. In practice, analytical models form the basis of numerical simulation studies and provide a comprehensive understanding of the reservoir behavior for the advanced studies.

The classic RTA and PTA analysis used for conventional reservoirs cannot be applied because they are generally developed to model early time flow regimes (Bilinear flow, Linear flow, Radial flow) that's followed by a late time flow regime (Boundary dominated

flow). The unconventional reservoirs, due to their extremely low permeability, tend to have transient flow (Bilinear flow regime, Linear flow regime) for very long durations. PTA requires the operator to shut-in the well for long durations (months or years) to allow the pressure transient to propagate in the extremely low permeability, which is economically unviable. The RTA analysis is capable of modelling variable rate with fixed BHP drawdown which can be closely achieved in the field. However, large noise due to surface activities, sub-surface fluid interaction and well completion strategies can lead to the analysis becoming extremely difficult to interpret. Further, the long-time BDF response required for RTA analysis may not be achieved in the life of the unconventional reservoir.

Development of the DTOF (τ) and the w(τ) Function

The Eikonal equation (1.1) is derived from the asymptotic (high frequency) limit of the diffusivity equation for the impulse pressure solution following (Vasco & Datta-Gupta, 1999) and (Kulkarni, Datta-Gupta, & Vasco, 2001).

$$\nabla\tau(x).\alpha(x).\nabla\tau(x) = 1 \tag{1.1}$$

Here, α denotes the hydraulic diffusivity:

$$\alpha = \frac{k}{\phi\mu c_t} \tag{1.2}$$

The DTOF is a generalization of the "radius of investigation" concept in a homogeneous reservoir. When extended to heterogeneous reservoirs, the DTOF captures the heterogeneity and governs the pressure front propagation (Datta-Gupta, Xie, Gupta, King,

& Lee, 2011). Figure 1 illustrates a comparison of the 'radius of investigation' in homogeneous reservoir and the DTOF in heterogeneous reservoir. The spatial heterogeneity in terms of porosity and permeability vanishes when the w(τ) function is introduced.

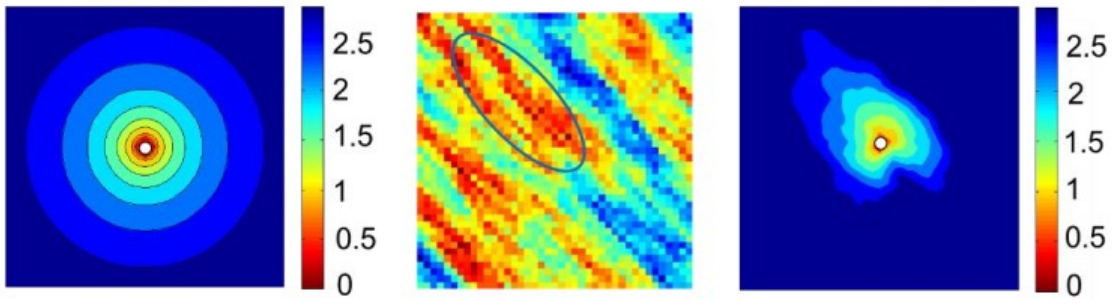

Figure 1: Examples of the pressure front propagation (a) Radius of investigation in homogeneous reservoir (b) Log permeability field (c) DTOF in heterogeneous reservoir (reprinted from Datta-Gupta et al. (2011))

Y. Zhang et al. (2016) first proposed to use the DTOF as a spatial coordinate to reduce the model and equations from 3D to 1D. The diffusivity equation in slightly compressible system, which can be expressed as:

$$\phi(\vec{x})c_t \frac{\partial p(\vec{x},t)}{\partial t} + \nabla.\vec{u} = 0 \tag{1.3}$$

$$\vec{u} = -\frac{1}{\mu}\vec{\vec{k}}(\vec{x}).\nabla p \tag{1.4}$$

A strong relationship is noticed between the pressure contours and τ contours which lets us assume that pressure gradients are aligned with the τ(x) gradients $p\left(\vec{x},t\right) \approx p\left(\tau\left(\vec{x}\right),t\right)$, we reduce the 3-D diffusivity equation to an 1-D form (King, Wang, & Datta-Gupta, 2016). The diffusivity equation is written in the form of a 1-D equation by using the definition of the Diffusive Time of Flight (τ) (Y. Zhang et al., 2014) :

$$\frac{\partial p}{\partial t} - \frac{1}{w(\tau)}\frac{\partial}{\partial \tau}\left(w(\tau)\frac{\partial p}{\partial \tau}\right) = 0 \tag{1.5}$$

Where,

$$w(\tau) = \frac{dV_p(\tau)}{d\tau} \tag{1.6}$$

Darcy's equation in τ coordinate is obtained as follows (King et al., 2016):

$$q \approx c_t w(\tau)\frac{\partial p}{\partial \tau} \tag{1.7}$$

Development of the Drainage Volume Analysis for Unconventional Reservoirs

For unconventional reservoirs, following Winestock and Colpitts (1965), and Song and Ehlig-Economides (2011), we use the rate normalized pressure (RNP) to calculate the drainage volume.

The well production is analysed based on the Rate Normalized pressure and its derivative. This represents the production behaviour observed if the well is produced at a constant

reference rate and is useful for identifying flow regimes. It is computed as (Song & Ehlig-Economides, 2011):

$$RNP = \frac{p_i - p_{wf}(t)}{q(t)} \tag{1.8}$$

$$RNP' = \frac{dRNP}{d\ln t_e} \tag{1.9}$$

The material balance time is defined as:

$$t_e = \frac{Q(t)}{q(t)} \tag{1.10}$$

The drainage volume may be calculated as:

$$\frac{1}{V_d(t)} \approx c_t \frac{d}{dt_e}\left(\frac{\Delta p_{wf}(t_e)}{q_w(t_e)}\right) \approx c_t \frac{d\,RNP(t_e)}{dt_e} \tag{1.11}$$

The drainage volume, pore volume and the w(τ) can be related as:

$$V_d(t) = \int_0^\infty d\tau . w(\tau) e^{-\frac{\tau^2}{4t}} = \int_0^\infty dV_p(\tau) e^{-\frac{\tau^2}{4t}} \tag{1.12}$$

Following J. Lee (1982), we may define the depth of investigation for an impulse source as the location of the maximum pressure drop within the reservoir. Based on the definition of well test derivative (1.13), at the limit $\left(\tau^2/4t\right) = 4$ where $e^{-\tau^2/4t} \approx 0.018$ the exponential term due to reflection from a barrier becomes appreciable compared to the value of unity, the value at τ = 0 (J. Lee, Rollins, & Spivey, 2003; Wang et al., 2019) . This limit is independent of the flow geometry, which makes it extremely useful in well test

interpretation. Here, we use the limit of detectability definition to determine the exponential term, $e^{-\tau^2/4t}$, which describes the relationship between the pore volume and the drainage volume (1.12).

$$\Delta p'(\tau,t) \equiv \frac{\partial \Delta p(\tau,t)}{\partial \ln t} \approx \frac{q_w}{c_t}\frac{t}{V(t)} e^{\frac{-\tau^2}{4t}} \tag{1.13}$$

This solutions are summarized in Figure 2 and Table 1 are important as they explain our ability to describe the fixed rate draw-down pressure transient problem, which is diffusive, as if the pressure was a wave with a front. The Boltzmann variable, $\xi = \tau^2/4t$, controls the solution characteristics for both homogeneous and heterogeneous reservoirs and in arbitrary dimensions (Yang, Sharma, Datta-Gupta, & King, 2015). For sufficiently small values, $\tau^2/4t < 0.01$ then $\exp(-\tau^2/4t) \approx 1$, and $\partial p/\partial t$ is independent of position τ. This is the pseudo steady state.

For $0.1 < \tau^2/4t < 4$, then $0.018 < \exp(-\tau^2/4t) < 0.9$, and $\partial p/\partial t$ depends on both τ and t. This is the pressure transient solution.

With large values, $\tau^2/4t > 4$, then $\exp(-\tau^2/4t) < 0.018$, and $\partial p/\partial t$ tends to zero which is the initial condition.

Table 1: Characteristics of the asymptotic pressure solution (reprinted from Wang et al. (2019))

Solution	Exponential Range	$\frac{\tau}{\sqrt{4t}}$ Range
Pseudo Steady State (PSS)	$e^{-\tau^2/4t} > 0.99$	$\frac{\tau}{\sqrt{4t}} < 0.1$
Transient	$0.99 > e^{-\tau^2/4t} > 0.018$	$0.1 < \frac{\tau}{\sqrt{4t}} < 2$
Limit of Detectability	$e^{-\tau^2/4t} = 0.018$	$\frac{\tau}{\sqrt{4t}} = 2$
Near Initial	$e^{-\tau^2/4t} < 0.018$	$\frac{\tau}{\sqrt{4t}} > 2$

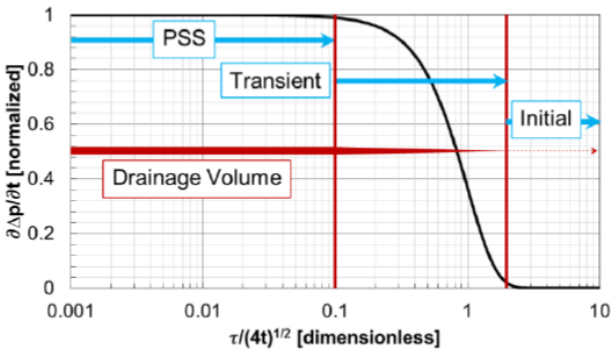

Figure 2: Spatial profile of the fixed rate drawdown solution to the asymptotic pressure approximation in terms of the time derivative of the pressure drop, normalized to its value at the wellbore (reprinted from Wang et al. (2019))

Dissertation Outline

In this dissertation, we focus to develop an application SPADES that can be used by an engineer to analyze wells and select refracturing candidates. We also focus on developing a production forecasting method for unconventional reservoirs.

In Chapter I, we introduce the background information about the fundamentals on the asymptotic approach of the diffusivity equation.

In Chapter II, we elaborate on the development of the application SPADES. A flow chart and a detailed explanation about the program is provided. Algorithms used for outlier removal, noise removal and selection of the number of splines is provided. The procedure used to automate these algorithms like by selecting optimized window length for Savitzky Golay and optimized knot selection for the basis function is explained.

In Chapter III, we discuss a production forecast method that is based on the transient analysis of this asymptotic solution. We model a fixed BHP flow for a simulated well and an Eagle Ford well. Sensitivity analysis for the parameters affecting the production forecast is also performed.

In Chapter IV, a discussion on possible future developments for this research project is presented. A conclusion to this study is presented and summarizing the outputs of the project

CHAPTER II

DATA DRIVEN PRODUCTION ANALYSIS AND DEVELOPMENT OF A COMPUTER APPLICATION - SPADES

Chapter Summary

Multistage hydraulically fractured wells have become an effective means of producing oil and gas from low permeability tight sand reservoirs. The completion technology used in these wells requires engineers to optimize parameters like the cluster spacing, proppant concentration, lateral length and well spacing. This further requires an understanding of the flow regimes and modelling of the reservoir pressure production response. The current industry practice for characterizing field behavior utilizes empirical decline curve analysis or pressure/rate transient analysis (PTA/RTA) for characterization of these reservoirs. These methods have inherent limitations due to their simplifying assumptions and do not provide a detailed description of the drainage volume evolution in the reservoir.

In this chapter, we implement the data-driven technology developed for the production rate and pressure analysis of shale oil and gas reservoirs. The work builds on previous studies for the diffusive time of flight, drainage volume analytics, refracturing candidate selection, data driven analytical workflow, optimized regularization techniques and development of the transient solutions (Datta-Gupta et al., 2011; Wang, 2018; Wang et al., 2019; Xue et al., 2019; Yang et al., 2015). This approach is based on

the high frequency asymptotic solution of the diffusivity equation in heterogeneous reservoirs.

A computer application was developed on a Python-Excel platform, this platform provides us with access to the Python scientific libraries and also lets us create a user-friendly Excel based interface. We elaborate on the problems associated with the previous implementation of the technique and the techniques used to improve the application.

The chapter describes the Outlier and noise removal techniques, Local Outlier Factor (LOF) and the Savtizky Golay algorithm, that are implemented to enhance the reservoir response while minimizing noise present in the field data. We also demonstrate techniques that automate the smoothening parameters used in these algorithms, this leads to consistent results and the user can focus on the results rather work on optimizing the smoothening parameters.

A detailed description of the Python-Excel code is also provided to assist in future development of the application. The chapter is organized as follows, first we discuss the motivation that lead us to build this application, then we provide the methodology that describes the algorithms and workflow of the application, and we end by providing a conclusion of our work.

Motivation

Industry adaptation required the development of a computer application that an engineer can use to evaluate well pressure-production data. The SPADES application was developed to provide an Excel based UI for analysis and optimization of hydraulic fractured wells in the tight sand reservoirs. It generates the drainage volume, w(τ) and IRR diagnostic plots, while also comparing multiple wells to select candidates for refracturing/ stimulation.

The initial version of this software was built on the Excel VBA platform and used the Fredholm inversion technique to calculate the w(τ) function. Further, Arp's decline was used to model the field production data which primarily modelled boundry dominated flow while wells in unconventional reservoirs are dominated by transient flow regime. This software required the following improvements for field applications:

Noise and Outlier Removal

The data-driven approach makes our results highly reliant on pressure production data. The data obtained from the field includes noise and outliers primarily because of miss reporting in the field, surface facility disturbances, tool failures etc. Outlier removal on the pressure production data needs to be performed before any diagnostic analysis. The presence of outliers in the data may result in incorrect identification of flow regimes, model well / reservoir and incorrect estimation of parameters of the model (Chaudhary & Lee, 2016).

The initial version of SPADES used Arp's Decline curve (Arps, 1945) based on the minimum square residual fit to model the pressure production trends. This leads to high smoothening of the data, however it was not an optimal choice for determining the pressure-production trend because the constants in Arp's hyperbolic decline equation for tight gas and shale wells, require values of b to be greater than unity, beyond the limit that Arps specified. With values of b equal to or greater than unity, the reserves derived using Arp's decline equation tend to have physically unreasonable properties (W. J. Lee & Sidle, 2010). The results are based on boundary dominated flow regime, rather than the transient flow regimes. Also, when a well flows with constant drawdown or constant BHP, it cannot capture the pressure-production profile (Figure 3).

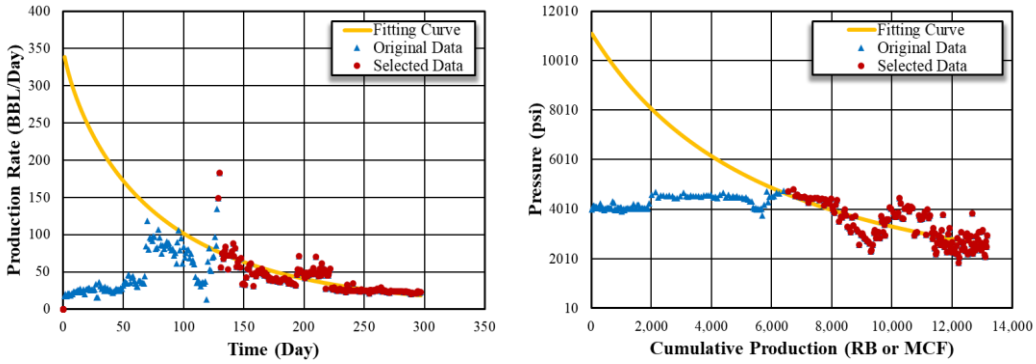

Figure 3: Arp's decline may not capture the original production profile

The production decline analysis techniques of Arps and Fetkovich only account for variations in bottom hole pressure during boundary-dominated flow and do not account

for such variations in the transient regime (Mishra, 2014). The Arp's decline determines the production and pressure trends individually, and cannot account for type curves based on Rate Normalized Pressure (RNP)

Algorithm for w(τ) Inversion

The drainage volume is calculated from the RNP and an inversion algorithm is used to calculates the w(τ). The initial version of SPADES modelled the drainage volume integral as a Fredholm integral equation (2.1)

$$V_d(t_i) = \sum_{j=1}^{N} \int_{\tau_{j-1}}^{\tau_j} e^{\frac{-\tau^2}{4t}} w(\tau) d\tau = \sqrt{\pi t_i} \sum_{j=1}^{N} w_j \left\{ erf\left(\frac{\tau_j}{2\sqrt{t_i}} \right) - erf\left(\frac{\tau_{j-1}}{2\sqrt{t_i}} \right) \right\} \quad (2.1)$$

Unfortunately, in this form, the inversion result is always unstable (oscillatory) because this problem is anti-diffusive and the matrix is near singular. Yang et al. (2015) provided a special treatment to the matrix elements along the main diagonal, to make the matrix semi-definite, which reduces the oscillation and the (τ) curve is improved (Figure 4). However, unphysical non-positive (τ) values may still be obtained. Further, the inversion is highly sensitive to the noise in the input data, so the input needs to be regressed using the Arp's decline curve based regression.

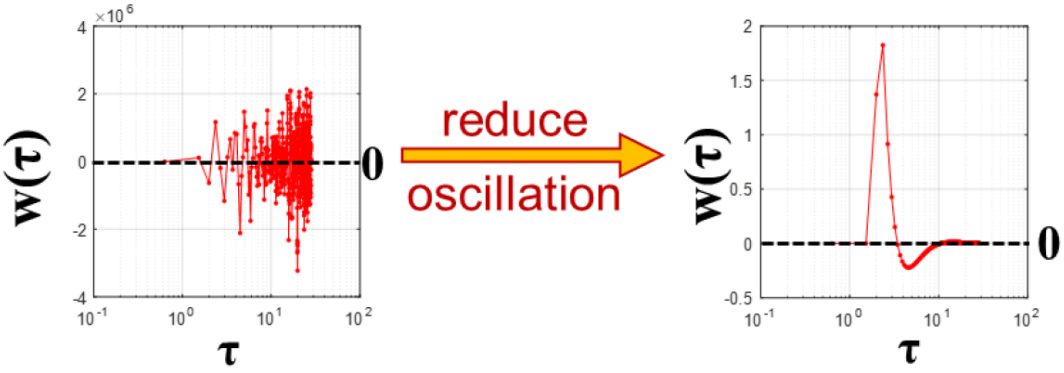

Figure 4: Illustration of reducing oscillation in the previous drainage volume inversion (reprinted from Yang et al. (2015))

Implementing the Fredholm integral does not provide an optimum representation of the linear flow regime and the identification of the fracture interference. Determination of reservoir properties from the w(τ) plot was inaccurate because of low resolution in the plot.

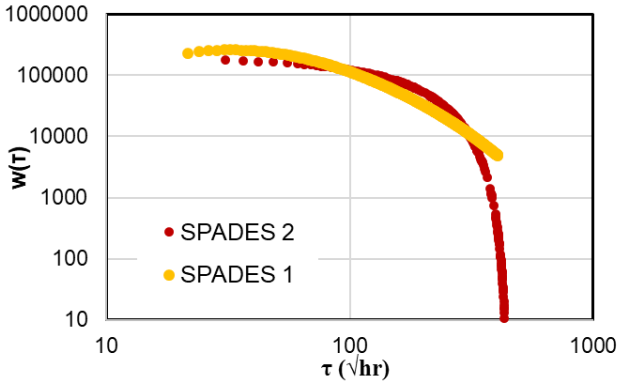

Figure 5: Low resolution and inaccurate identification of fracture interference in previous version of SPADES

Selection of Programming Platform

The initial version of SPADES uses Excel VBA as the primary platform of development. This platform has limited array based calculations, it lacks standard scientific programming libraries and is slow in terms of computation speed. This limits the application of software for $w(\tau)$ inversion using the 4^{th} order splines and convex optimization.

Oilfields with large number of wells required multi well user interface which makes the analysis computationally intensive and can cause large lags due to the use of VBA.

Methodology

The asymptotic analysis leads to the Eikonal equation that describes the evolution of the drainage volume accounting for reservoir heterogeneity and complex fracture geometry. Using numerical solution of the Eikonal equation, we have also developed an application to understand the reservoir performance. The workflow improves the noise, outlier removal techniques and calculates the well drainage volume, $w(\tau)$ and IRR directly from the well production data without resorting to geologic modeling and flow simulation. The $w(\tau)$ function is the diagnostic tool and gives us more insight into reservoir and fracture flow geometry compared to the traditional PTA/RTA.

Workflow of the SPADES Application

The application uses two methods to smoothen the data: LOF-Savitzky Golay based outlier - noise removal and the Arp's decline curve method (Figure 6) . The default option

is the Outlier – Noise removal method, however the Arp's decline curve method provides backward compatibility with the previous version of SPADES. The Outlier-Noise removal method uses automation techniques and requires little effort from the engineer towards optimizing the Outlier-Noise removal.

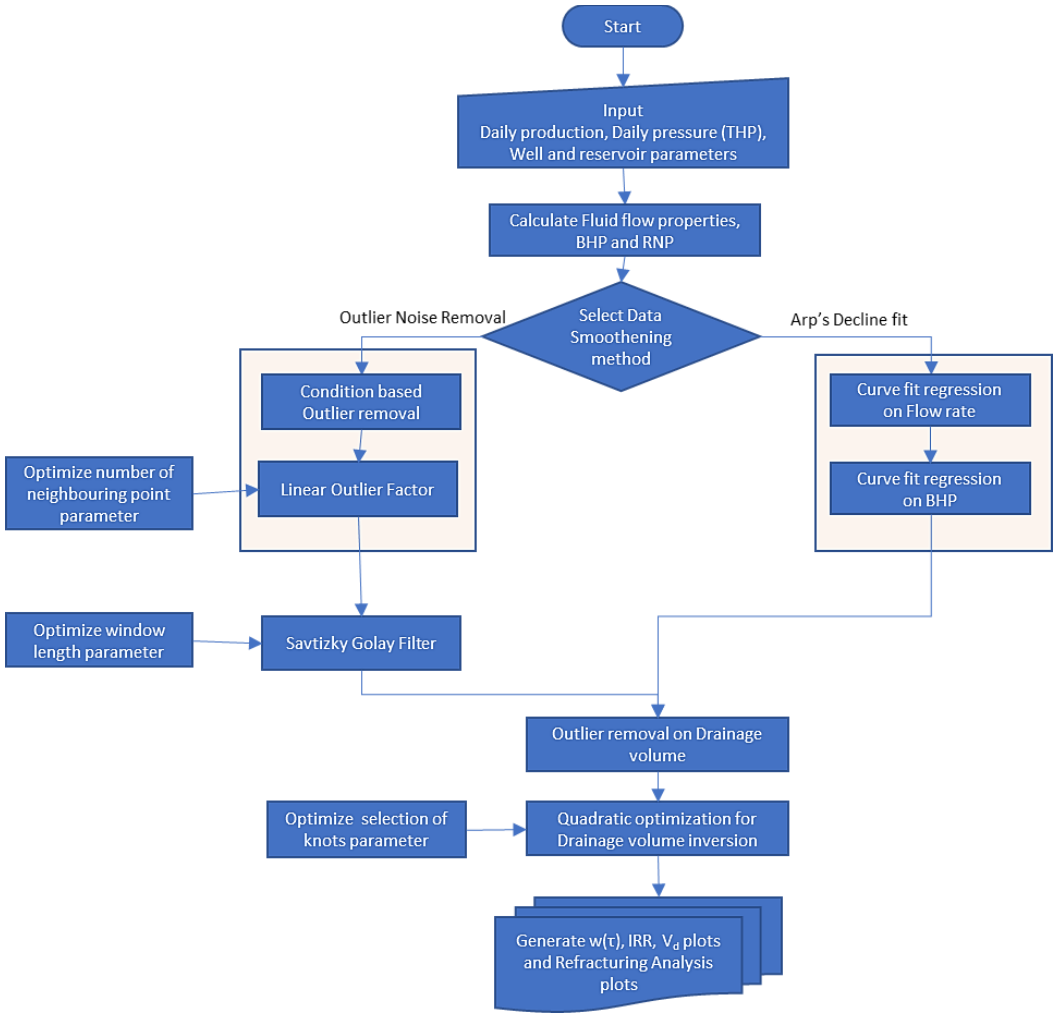

Figure 6: Flowchart of the SPADES application

The UI components like data input, calculation mode selection and display of results are made available in Excel, while the data processing and results are generated in Python. Xlwings, a python library, is used to transfer data between Python and Excel.

Outlier Removal

The goal for Outlier detection is to separate a core of regular observations from some abnormal ones. We use condition based outlier filters to screen the data before implementing the LOF Algorithm. The conditional filters are:

- Duration of flow is zero: Indicates shut in period and needs to be removed as they may lead to very Rate normalized pressure and material balance time values
- Material balance time is negative: The material balance time becomes negative when the flow rate is reported as negative. This rarely happens and generally is due an error with measuring/reporting data.
- Remove data point with large difference between t_e and time: This removed points above a threshold for $t_e/time$, to exclude very large t_e values. This condition occurs when the flow rate is very low.
- Remove negative data for RNP: The reservoir pressure is expected to drop with production, however, miss reporting may lead to BHP higher than the initial reservoir pressure. This may also occur when an adjacent well is fracked.

Local Outlier Factor

The LOF algorithm computes the local density of an observation, and declares it an outlier if it has substantially lower density than its neighbors. The algorithm does not require any training dataset and is an unsupervised outlier detection method. Rate/pressure data are reported at different frequencies like monthly, daily and the material balance time may further change the density of data points. However, the LOF algorithm can be used for our application because it considers how isolated an observation is from its neighbors and not the overall dataset.

The LOF score of an observation is equal to the ratio of the average local density of his k-nearest neighbors, and its own local density: a normal instance is expected to have a local density similar to that of its neighbors, while abnormal data are expected to have much smaller local density ("Novelty and Outlier Detection — scikit-learn 0.23.1 documentation,").

Chaudhary and Lee (2016) provide a detailed discussion of the LOF algorithm. Here, we explain a few concepts from their work that help us understand the formulation of this algorithm.

The reachability – distance of an object p from o is defined as the true distance between the two objects, but at least the k – distance of object o. The local reachability density (lrd) of an object p is defined as the inverse of the average reachability distance of the object p from its k nearest neighbors (2.2).

$$lrd_k(p) = 1 \Bigg/ \left(\frac{\sum_{o \in N_{k(p)}} reachability - dis\tan ce_k(p,o)}{|N_k(p)|} \right) \tag{2.2}$$

The LOF of an object is the average lrd of its neighbors divided by the object's own lrd. Therefore, LOF captures the degree to which we call the object an outlier.

$$LOF_k(p) = \frac{\sum_{o \in N_k(p)} \left(\frac{lrd(o)}{lrd(p)} \right)}{|N_k(p)|} = \left(\frac{\sum_{o \in N_k(p)} lrd(o)}{|N_k(p)|} \right) \Bigg/ lrd(p) \tag{2.3}$$

An output of implementing this outlier removal workflow is presented in Figure 7. The abnormally high RNP and t_e values have been filtered which prepares the data set for further smoothening using the Savitzky Golay algorithm. The number of k-neighbours is kept constant at twenty because that represents almost a month of observations and this is also recommended by Chaudhary and Lee (2016)

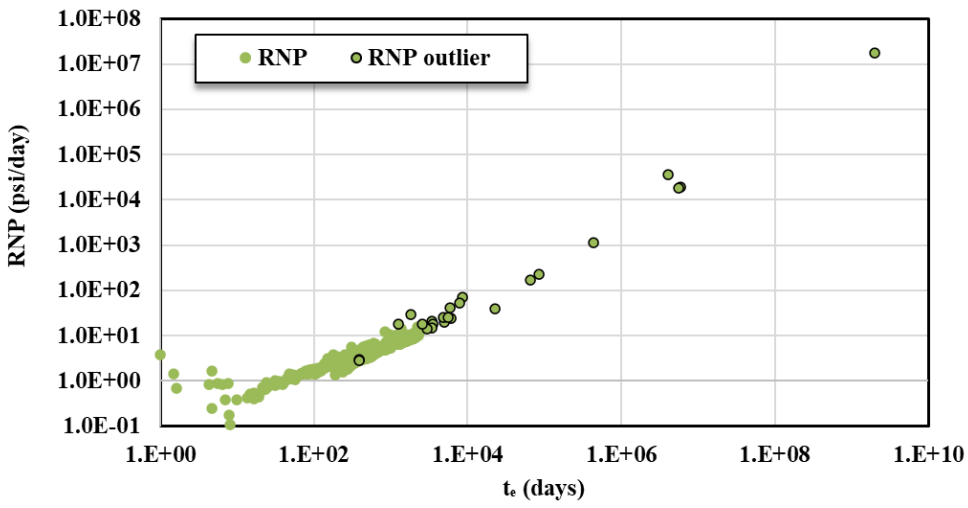

Figure 7: Outlier identified in the RNP values of an oil well. The log-log axis makes the initial points seem like outliers, but they are not.

Noise Removal: Savitzky Golay Filter

In field cases, the pressure-production data is influenced by many variables like change in fluid property, flow regime, surface equipment and adjacent well activities. The dataset is generally represented as: True Model+ Noise+ Outliers. In our approach, true model represents the reservoir response, and should follow a smoother trend. Noise is the distortion in the true model that has a higher density of neighbouring observations as compared to outliers.

A Savitzky–Golay filter uses a process known as convolution where successive sub-set of adjacent data points are fit with a low-degree polynomial by the method of linear least squares (J. Zhang, Zou, & Tian, 2017). Savitzky and Golay (1964) showed that a set of data points could be derived and used as weighting coefficients to carry out the smoothing

operation. These weighting factors are exactly similar to polynomial curve fit factors. Therefore, the smoothed data points (Y) from the Savitzky-Golay algorithm for a set of m convolution coefficients (C_i) is given by the following equation:

$$Y_j = \sum_{i=-(m-1)/2}^{i=(m-1)/2} C_i y_{j+i} \tag{2.4}$$

Sadeghi and Behnia (2018) recommended the method to select the length of the sliding window for the Savitzky Golay algorithm. For a dataset with variance σ^2, the Savitzky-Golay filter with order n and optimum window length (N_{opt})is defined as,

$$N_{opt} = {}^{2n+5}\sqrt{\frac{2(n_{SG}+2)((2n_{SG}+3)!)^2}{((n_{SG}+1)!)^2}\frac{\sigma^2}{\upsilon_n}} \tag{2.5}$$

Here,

$$\upsilon_n = \frac{1}{L}\sum\nolimits_t \left(f^{(n+2)}(t)\right)^2 \tag{2.6}$$

The value of RNP obtained after noise removal is used to calculate the drainage volume. It provides a smooth value as shown in Figure 8.

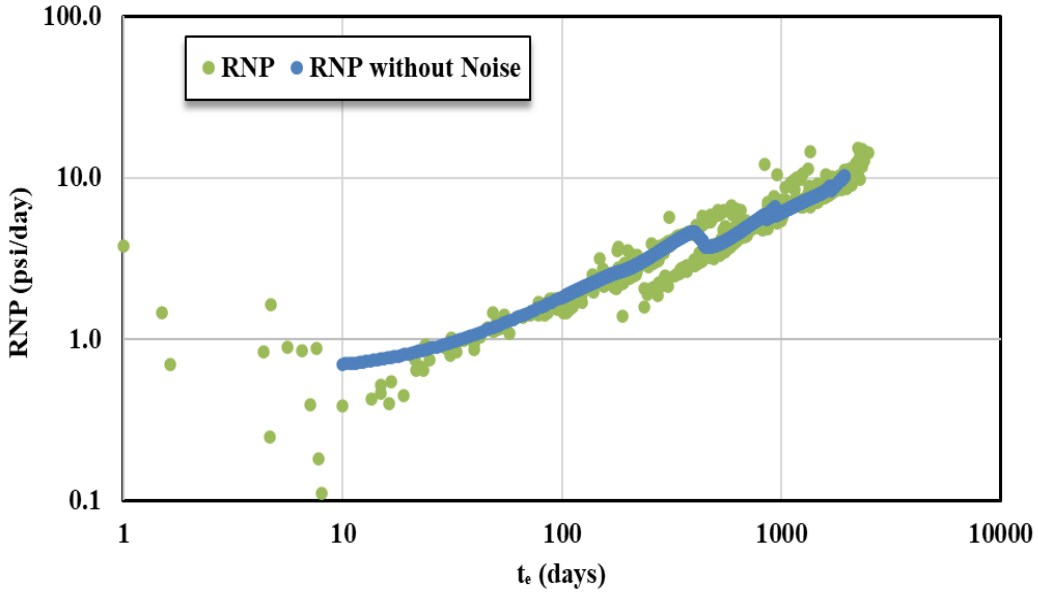

Figure 8: RNP obtained from the noise removal workflow that implements the Savitzky Golay filter

*Regularized Least Squares Optimization**

The drainage volume inversion (1.12) is treated as an optimization under constraints to yield positive and smooth w(τ) values. This also improves the w(τ) previously calculated by a Fredholm integral and also provides a better resolution in the w(τ) plots (Figure 5).

Wang et al. (2019) provides a detailed discussion of this method. Here, we present the algorithm used in the application. The w(τ) is approximated using 4th order B-spline basis functions that we generate using the *bspline* library in Python.

$$V_d \approx \int_0^{\infty} e^{\frac{-\tau^2}{4t}} w(\tau) d\tau \quad where \quad w(\tau) = \sum_{k=1}^{n_{basis}} \alpha_k \phi_k(\tau) \tag{2.7}$$

The objective function (2.8): the first term represents the residual sum of errors, the second term is a roughness penalty used to guarantee curve smoothness subject to a non-negative $w(\tau)$ constraint (Wang et al., 2019). This convex optimization is performed using the *cvxopt* library in python.

---

*Reprinted with permission from "Quantitative production analysis and EUR prediction" from unconventional reservoirs using a data-driven drainage volume formulation" by Zhenzhen Wang, Andrew Malone, Michael J. King, 2018. Computational Geosciences, Copyright 2019 by Springer Nature Switzerland AG.

$$\min_{\alpha} \frac{1}{2}\alpha^T (A^T A + \lambda M)\alpha - V^T A\alpha + \frac{1}{2}V^T V \quad Subject\ to\ w(\tau) \geq 0 \tag{2.8}$$

$$\text{Where} \quad A_{ij} = \int_0^{\infty} \phi_j(\tau) e^{\frac{-\tau^2}{4t_i}} d\tau \quad M_{ij} = \int_0^{\infty} \phi_i''(\tau)\phi_j''(\tau) d\tau \quad V = \left[V_1, V_2, ..., V_{n_t}\right]^T \tag{2.9}$$

All $\tau_j's$ are generated with the detectability condition as: $(2\tau_j)_2/4t_j = 4 \Rightarrow \tau_j = 2\sqrt{t_j}$. The roundtrip time is t_j for pressure front to propagate from the well to location τ_j, and back again.

The B-splines generated for this method use the number of knots as a tuning parameter. In order to optimize the number of knots, we need to understand how good the model is able to match the actual data and how complicated does the model have to be. Higher number of knots may lead to overfitting while a smaller number of knots may lead to under fitting. We used probabilistic model selection methods, AIC and BIC, because it does not require a test dataset, all of the data can be used to fit the model, and can be scored directly (Dziak, Coffman, Lanza, Li, & Jermiin, 2019). The AIC and BIC are penalized likelihood criteria that indicate how close the model is to the true model while penalizing for the number of parameters.

$$AIC = n\ln(\sigma^2 / n) + 2K \tag{2.10}$$

$$BIC = n\ln(\sigma^2 / n) + 2K\ln(n) \tag{2.11}$$

Dziak et al. (2019) show that AIC and BIC may not be used individually as AIC always has a chance of choosing too big a model while BIC has very little chance of choosing too small a model. So, it is recommended to use AIC and BIC together in model selection.

The AIC BIC parameters are calculated for different knot sizes : $1/3, 1/6, 1/10, 1/15, 1/20, 1/30$ th of the number of datapoints and the value with the lowest AIC, BIC values is selected.

Xlwings: Discussion

Xlwings is an open source Python library that provides an API to interface between Python and Ms Excel. This allows us to have an Ms Excel based user interface while Python is used in the back end for calculations. Implementing python provides access to scientific libraries like NumPy, SciPy for implementing Outlier removal algorithms, Noise removal algorithms and convex optimization based solutions.

Xlwings and other scientific modules in python can be deployed without any installation procedures. This is accomplished by using the PyInstaller tool to compile all the Python modules into a directory or an executable. This helps the user in a company conform to IT policies that may block the use of certain file types and installation procedures.

With a multi-well interface, the user can have an automated input mechanism. Text based files are considered an industry standard form of data input and are easily handled by most programming languages.

Conclusions

In this chapter, we describe the development of an application SPADES that is used to implement the w(τ) based diagnostic approach. The implementation uses Xlwings as an interface between Python and Excel. Some key conclusions for this paper are summarized as follows:

The workflow for the SPADES application implements an automated Outlier-Noise detection method and also the Arp's decline curve fit method, giving user an option to choose either. A flowchart depicting the structure of the code is also presented.

We demonstrate the importance and use of Outlier-Noise removal algorithms used in the application. In the Local Outlier Factor method, the k-neighbours are set to a fixed value as recommended by Chaudhary and Lee (2016). An algorithm developed by Sadeghi and Behnia (2018) is used to select the window length for Savitzky Golay filter. Probabilistic model selection methods, AIC and BIC, are used to optimize the number of B-spline knots for the Regularized Least Squares Optimization.

CHAPTER III

APPLICATIONS OF THE DIFFUSIVE TIME OF FLIGHT TO A DATA DRIVEN APPROACH FOR DECLINE CURVE ANALYSIS*

Chapter Summary

The transient linear flow regime dominates the production behaviour for unconventional reservoirs. The time scale for a transient response is orders of magnitude greater than in higher permeability conventional reservoirs and requires development of techniques akin to rate transient analysis (RTA) that can capture the reservoir behavior over its producing life (King et al., 2016).

Analytical methods provide a physical basis to production forecasting and also more reliable results than current empirical methods like Arp's decline, Duong decline, stretched exponential and power law. This method presented here provides data driven approximation of reservoir properties like matrix permeability, fracture area and fracture half length. The method bounds the forecast by the pore volume and provides us with an estimation of the UR.

---

*Reprinted with permission from "Applications of the Diffusive Time of Flight to a Data Driven Approach for Decline Curve Analysis" by Ankit Bansal, Michael J. King, 2020. Paper urtec-2020-3076 is to be presented at Unconventional Resources Technology Conference, 2020, Austin, Texas, USA by Ankit Bansal

In the current study, an asymptotic analysis of the diffusivity equation is extended to decline curve analysis. This asymptotic solution was introduced in the first chapter and it characterizes the transient drainage volume and drainage geometry of the wells (King et al., 2016). This approach was further used to identify fracture interference, optimize completion design and select re-fracturing candidates (Yang et al., 2015).

The chapter begins by outlining the motivation to develop this technique. Then we develop the concept of transient flow based on the asymptotic solution of the diffusivity equation. Here, the concepts of time of flight (τ), drainage volume (V_d) and $w(\tau)$.are extended towards defining the transient solutions of infinite and bounded reservoirs, which form the basis for production forecast. The workflow to implement the algorithm is then described and the validated on a simulation model with an infinite conductivity, multi-fractured well. Further, we implement the technique to make a production forecast in an Eagle ford well and compare the results to the Duong's decline curve method. Further, sensitivity analysis is performed to identify uncertainties with impact on the results. Finally, we end with a discussion and conclusions for our work.

Motivation

Traditional decline methods such as Arp's rate/time relations and its variations do not work for wells producing from tight sand or shale reservoirs in which fracture related flow is dominant (Duong, 2011). The development of drainage volume formulation using the diffusive time of flight has shown that hydraulic fractured wells produce beyond linear flow regime and may have boundary-dominated flow.

The Arp's hyperbolic decline curve models the transient behavior using $b \geq 1$. However, this value of 'b' is not a physically reasonable and may result in unrealistic properties (W. J. Lee & Sidle, 2010). The EUR may be kept bounded by imposing an exponential decline with a minimum decline rate, however, this also does not have a physical basis to it (W. J. Lee & Sidle, 2010).

The Duong's method provides an accurate implementation for transient linear flow by providing a power law relationship between production rate and time (2.12) (Duong, 2011). This leads to a straight line on a log - log plot until the Boundary Dominate flow is reached (Kanfar & Wattenbarger, 2012). This method uses 'm' as the empirical fitting parameter that fails to have a physical basis. As the flow regime changes over the life of a well, this method tends to overestimate the EUR (Okouma Mangha, Ilk, Blasingame, Symmons, & Hosseinpour-zonoozi, 2012).

$$\frac{q}{Q} = at^{-m} \tag{2.12}$$

The Power law model can model the change from linear flow to boundary dominated flow by considering the decay to be power function. However, it leads to non-unique solutions because of large degrees of freedom resulting from the unknown parameters (Ali & Sheng, 2015). Stretched Exponential Decline model requires solving complex non-linear equations and is recommended for large scale evaluation of fields (Ali & Sheng, 2015; Tan, Zuo, & Wang, 2018; Wang, 2018, p. 113). Each of these decline curve models have their own strengths, however, each of these models can only be described as empirical,

and there is no direct link with reservoir engineering theory, other than via analogy (Okouma Mangha et al., 2012).

The current Decline curve models are empirical and use a ‘best-fit’ curve to model well behaviour. These techniques have inherent validity and applicability issues because of their empirical nature. Analytical methods like the Fetkovich type curves and Material balance techniques are not appropriate for unconventional reservoirs as they model boundary-dominated flow where the well may be producing under pseudo steady state or steady state flow regime.

For hydraulically fractured wells in shale reservoirs that have boundary dominated flow, Duong’s decline overestimates the EUR. We impose exponential decline on the Hyperbolic Arp’s decline to avoid over estimation of the EUR because the hyperbolic solution may never converge to zero. The pore volume contributing to Well production should bound the EUR. The Arp’s model and Duong’s model are simple and fast, however they tend to over predict the EUR for unconventional reservoirs. Extended models like the Power Law Exponential Decline Model have many unknowns with multiple acceptable solutions, Stretched Exponential Decline model requires solving complex non-linear equations (Tan et al., 2018).

Traditional decline curve methods provide production rate history match and forecast information. It bases the regression parameters on ‘best-fit’ curve and are not dependent on reservoir properties. Almost no information is obtained about the well and reservoir during the analysis. Unconventional reservoir behaviour is largely influenced by the

fracture half length, matrix permeability, area of fracture which are not available from conventional decline curve analysis.

Background

For unconventional reservoirs, following Winestock and Colpitts (1965), and Song and Ehlig-Economides (2011), we may use the rate normalized pressure (RNP) to calculate the drainage volume. This RNP approximation represents the production behavior that would be observed if the well were produced at a constant reference rate.

The mixed form of the diffusivity equation, (1.5) and (1.7), is used in the solution for the asymptotic pressure approximation (King et al., 2016), and it allows us to develop closed form solutions.

$$c_t \frac{\partial \Delta p}{\partial t} = -\frac{1}{w(\tau)} \frac{\partial q}{\partial \tau} \approx A(t).K(\tau, t) \tag{2.13}$$

Here, K(τ,t) is the diffusion kernel defined based on the inner and outer boundary conditions (Table 2). Depending upon the boundary conditions, the equation for A(t) may be algebraic or it may be an Ordinary Differential Equation (ODE). The approximations to the kernels for bounded systems should always have an odd number of terms, since every pair of terms are of the same magnitude at the inner boundary- where we will measure and reference the solution. Although bounded systems require an infinite number of terms for an exact solution, the current solution methodology provides excellent approximations with the three terms shown.

A detailed description of transient analysis is provided in Wang et al. (2019). Here, we provide a brief description of the concepts used in the analysis. We discuss the BDF solutions to determine the productivity index and pressure-production solution for fixed BHP drawdown.

Table 2: Diffusion kernels for different inner and outer boundary conditions (Wang et al., 2019)

$K(\tau, t)$	Infinite domain	Bounded reservoir: no flow at $\tau = \tau_{res}$
Fixed rate at $\tau = 0$	$e^{-\tau^2/4t}$	$e^{-\tau^2/4t} + e^{-(2\tau_{res}-\tau)^2/4t} + e^{-(2\tau_{res}+\tau)^2/4t} + +...$
Fixed BHP at $\tau = \tau_{wf}$	$\frac{(\tau-\tau_{wf})}{\sqrt{4t}} e^{-\frac{\tau^2}{4t}}$	$\frac{(\tau-\tau_{wf})}{\sqrt{4t}} e^{-\frac{\tau^2}{4t}} + \frac{(2\tau_{res}-\tau-\tau_{wf})}{\sqrt{4t}} e^{-\frac{(2\tau_{res}-\tau)^2}{4t}} - \frac{(2\tau_{res}+\tau-3\tau_{wf})}{\sqrt{4t}} e^{-\frac{(2\tau_{res}+\tau-3\tau_{wf})^2}{4t}} - +...$

$$V(\tau,t) \equiv \int_{\tau}^{\infty} d\tau w(\tau) K(\tau,t) \text{ and } V(t) \equiv V(\tau_{res},t) \tag{2.14}$$

$$W(\tau,t) \equiv \int_{\tau_{wf}}^{\tau} \frac{d\tau'}{w(\tau')} \{V(t) - V(\tau',t)\} \text{ and } W(t) \equiv W(\tau_{res},t) \tag{2.15}$$

$$X(\tau,t) \equiv \int_{\tau_{wf}}^{\tau} d\tau' w(\tau') W(\tau',t) \text{ and } X(t) \equiv X(\tau_{res},t) \tag{2.16}$$

Transient Analysis: Bounded Reservoirs with Fixed Rate or Fixed BHP

The bounded reservoir cases we will examine have a no-flow outer boundary at $\tau = \tau_{res}$ and either fixed rate or fixed-BHP boundary conditions at the wellbore, $\tau = 0$. Again, the solution will be expressed for an arbitrary geometry.

$$q(\tau,t) = q_w(t) \left\{ 1 - \frac{V(\tau,t)}{V(t)} \right\} \tag{2.17}$$

$$\Delta p(\tau,t) = \Delta p_{wf}(t) - \frac{q_w}{c_t}\frac{W(\tau,t)}{V(t)} \tag{2.18}$$

Further, we can relate the pressure solution to the average reservoir pressure drop, which is itself related to the cumulative production and pore volume of the reservoir.

$$\overline{\Delta p}(t) = \frac{Q_w(t)}{c_t.V_{res}} \qquad Q_w(t) = \int_{t'=0} dt' q_w(t') \qquad V_{res} = \int_{\tau=0}^{\tau_{res}} w(\tau) d\tau \tag{2.19}$$

We can also relate the solution to the well productivity, *J (t)*. However, just as the definition of the drainage volume was extended from PSS to transient, this is a transient extension for the well productivity. This expression will clearly reduce to a constant well productivity in the long time limit.

$$\frac{1}{J(t)} \equiv \frac{\Delta p_{wf} - \overline{\Delta p}}{q_w} = \frac{1}{c_t.V_{res}}\frac{X(t)}{V(t)} \tag{2.20}$$

Rate Transient Analysis: No-Flow Outer Boundary Reservoir with Fixed-BHP Drawdown

This case has a variable flow rate so that $q_w(t) = dQ_w / dt$. Flowing material balance time equation leads to an ODE for cumulative production.

$$\frac{1}{J(t)}\frac{dQ_w}{dt} + \frac{1}{c_t.V_{res}}Q_w = \Delta p_{wf} \tag{2.21}$$

The solution may be expressed in terms of material balance time, t_e

$$RNP_{wf}(t) = \frac{\Delta p_{wf}}{q_w(t)} = \frac{t_e}{c_t.V_{res}} + \frac{1}{J(t)} \quad where \quad t_e = \frac{Q_w}{q_w} \tag{2.22}$$

In the long time limit where $J(t) \to J_{BDF}$, and we recover an solution with exponential decline rate of $D = \frac{J_{BDF}}{c_t . V_{res}}$. This is the Arp's b=0 solution

Methodology

Here we explain the workflow to implement this technique for a well producing from a very low permeability reservoir.

Outlier and Noise Removal

Pressure and Production data generally includes noise and outliers. The Rate Normalized Pressure (RNP) is calculated and filtered to represent the actual reservoir response and the drainage volume of the well. This step has been discussed in Chapter II and is an important part of the SPADES application,

Regularized Least Squares Optimization for Drainage Volume Inversion

The *w(τ)* is approximated using a 4th-order B-spline basis functions, and the drainage volume expression is discretized as follows:

$$V_d(t) \equiv \int_0^\infty e^{-\frac{\tau^2}{4t}} w(\tau) d\tau \quad where \quad w(\tau) = \sum_{k=1}^{n_{basis}} \alpha_k \phi_k(\tau) \tag{2.23}$$

where φ_k is the basis function and the α_k is its coefficient, which is unknown. This method has been discussed in Chapter II and is used to obtain the w(τ) values for diagnostic plots.

Calculate the Reservoir Properties and Well Completion Parameters

Fracture interference occurs when the drainage volumes from each fracture begins to overlap, i.e., at the stagnation line between fractures. Fracture interference generally occurs within the first three to six months.

The rate of increase in drainage area drops significantly due to fracture interference, which is reflected in the sudden drop of w(τ) and defines the τ_{elf}. We will use this value of τ_{elf} to estimate the diffusivity and matrix permeability.

From the definition of Diffusive Time of Flight (τ) and diffusivity (Wang et al., 2019) ,

$$\tau_{ifi} = \frac{x_s}{2\sqrt{\alpha}} \quad where, \quad \alpha = \frac{k}{\phi \mu c_t} \tag{2.24}$$

$$k_m = \left(\frac{x_s}{2\tau_{ifi}} \right)^2 \phi \mu c_t \tag{2.25}$$

The fracture area is defined from the pore volume of the fractures that contribute to the initial linear flow regime. The value of w(τ) during linear flow is used to calculate the fracture area and fracture half length:

$$V_{p,BDF}(r) = n\pi r(x_f + r)h\phi \tag{2.26}$$

$$V_{p,BDF}(\tau) = n\pi\tau\sqrt{\alpha}(x_f + \tau\sqrt{\alpha})h\phi \tag{2.27}$$

$$w(\tau) = \frac{\partial V_{p,BDF}}{\partial \tau} = A_f\sqrt{\alpha\phi} + 2n\pi h\phi\tau\alpha \quad where, \quad A_f = n\pi x_f h \tag{2.28}$$

$$A_f = \frac{w(\tau_{lf})}{\sqrt{\alpha\phi}} \tag{2.29}$$

$$x_f = \frac{A_f}{\pi n_f h} \tag{2.30}$$

Forecast the w(τ) Function

The multi-stage hydraulic fractured well is expected to have an elliptical drainage volume (Figure 9). We consider an infinite conductive, fully penetrating, planar hydraulic fracture that has fluid flow in a 2-D porous medium.

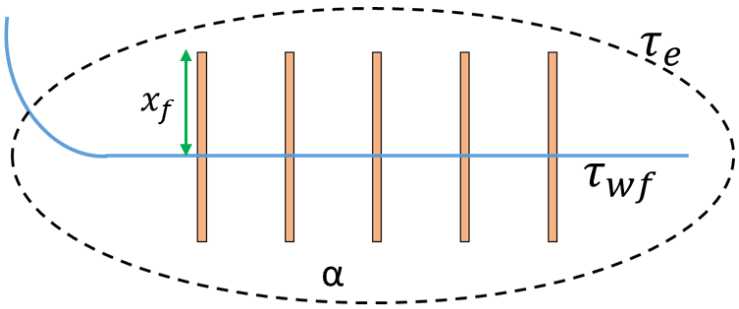

Figure 9: Graphical representation of multi-fractured horizontal well and its elliptical drainage volume (Reprinted with permission from Ankit Bansal and King (2020))

The pore volume for an ellipsoidal drainage volume is calculated from the fracture half-length and diffusivity coefficient calculated from the previous step. The w(τ) is the derivative of the pore volume and is a linear function of τ, which can be extended to τ_e.

$$V_p(r) = \pi\phi h(l/2 + r)(x_f + r) \tag{2.31}$$

$$\tau_e = \frac{r}{\sqrt{\alpha}} \tag{2.32}$$

$$V_p(\tau) = \pi\phi h\left(l/2 + \tau\sqrt{\alpha}\right)\left(x_f + \tau\sqrt{\alpha}\right) \tag{2.33}$$

$$w(\tau) = \frac{\partial V_p}{\partial \tau} = \sqrt{\alpha}\pi h\phi\left(x_f + l_w/2 + 2\tau\sqrt{\alpha}\right) \tag{2.34}$$

Production Forecast

The reservoir volume with a no flow boundary represents the elliptical drainage volume. The well productivity is defined by the Bounded reservoir transient analysis:

$$\frac{1}{J(t)} \equiv \frac{\Delta p_{wf} - \overline{\Delta p}}{q_w} = \frac{1}{c_t.V_{res}} \int_{\tau=0}^{\tau_{res}} \frac{V_{res}(\tau,t)}{w(\tau)} \left\{1 - \frac{1}{PV} \int_{\tau'=0}^{\tau} w(\tau')d\tau\right\} d\tau \tag{2.35}$$

The cumulative production volume and daily production rate is determined from the Rate transient analysis implementation for bounded reservoir,

$$\frac{1}{J(t)}\frac{dQ_w}{dt} + \frac{1}{c_t.V_{res}}Q_w = \Delta p_{wf} \tag{2.36}$$

Solving the ODE for Q_w,

$$Q_w = \frac{1}{v(t)}\left[\int_0^{t_e} v(t)\Delta p_{wf} J(t)dt + c\right] \quad where, \; v(t) = e^{\int_0^t \frac{J(t)}{c_t V_{res}}} \tag{2.37}$$

$$q_w = \frac{\partial Q_w}{\partial t} \quad and \quad t_e = \frac{Q_w}{q_w} \tag{2.38}$$

The solution may be expressed in terms of material balance time (t_e),

$$RNP_{wf}(t) = \frac{\Delta p_{wf}}{q_w(t)} = \frac{t_e}{c_t.PV} + \frac{1}{J(t)} \tag{2.39}$$

This expression is closely related to the expression for the rate-normalized pressure drop for a fixed-rate BHP, although the diffusion kernels are different in these two cases. If we approximate superposition time by material balance time, this solution provides the following approximate expression for the transient drainage volume:

$$\frac{1}{V_d(t_e)} \approx c_t \frac{dRNP_{wf}}{dt_e} = \frac{1}{PV} + c_t \frac{d}{dt_e}\left(\frac{1}{J(t)}\right) \tag{2.40}$$

The drainage volume reduces to the pore volume of the system once the transient terms become negligible.

Illustration of Methodology

We implement this workflow to a simple model: a well with infinite conductivity fractures in a low permeability reservoir. We use a tartan grid to model the reservoir with hydraulic fractures (Figure 10). These fractures fully penetrate the thickness of the reservoir. To provide better resolution, the grid size gradually reduces in the X direction as we move close to the fractures. The grid size is uniform in the Y and Z directions. The well produces at a constant BHP of 3000 psi. Other key parameters are summarized in Table 3. Outlier removal and noise reduction is not required because the results are generated from a finite element simulator.

Table 3: Reservoir, fluid, and wellbore properties of the simulation model (Reprinted with permission from Ankit Bansal and King (2020))

Property	Value	Unit
h	250	ft
L_{res}	718	ft
w_{res}	305	ft
x_f	102.5	ft
k	2E-4	md
ϕ	0.06	
μ	0.2	cp
c_t	3E-5	psi^{-1}
B	1	rb/bbl
r_w	2.76	ft
L_{well}	437	ft
Δp_{wf}	3000	psi
t_{prod}	2500	days

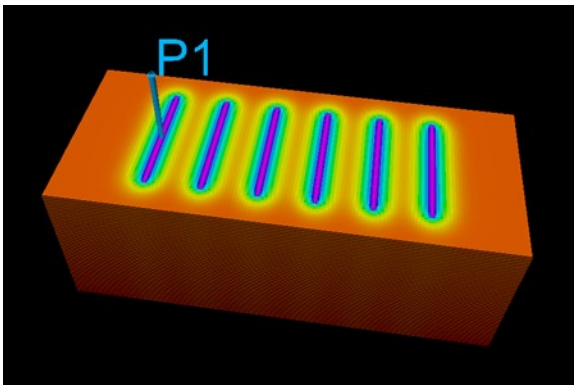

Figure 10: Eclipse model of the MFHW (Reprinted with permission from Ankit Bansal and King (2020))

The intiation of fractue interference is at τ_{ifi}= 21 √day identified by the initiation of significant drop in w(τ). It is used to determine reservoir parameters k_m, α, A_f and x_f. The results (Table 4) are similar to the model inputs and the variation is due to the uncertianily associated with determining the τ_{ifi}. This uncertainity is very small as compared to values obtained from other diagnostic plots (Wang et al., 2019). Also, τ_e is used in the diffusion kernel as well as the upper limit of integration for the bounded reservoir solutions.

Table 4: Reservoir parameters derived from the asymptotic solution with simulation model inputs (Reprinted with permission from Ankit Bansal and King (2020))

Property	Model Input	Derived from the Asymptotic Solution	Unit
k_m	2E-4	2.5E-04	mD
α	3.5	4.4	ft^2/day
A_f	6.2E+5	6.63e+05	ft^2
x_f	102.5	108.4	ft

In Figure 11, w(τ) is extended for an elliptical drainage volume till τ_e =. 50 √days. We use the production data derived w(τ) to model linear flow regime and later transition to an elliptical drainage volume based w(τ) for production forecast. The drainage volume (V_d) and the w(τ) calculated from the simulation and forecasted based on w(τ) is presented in Figure 12.

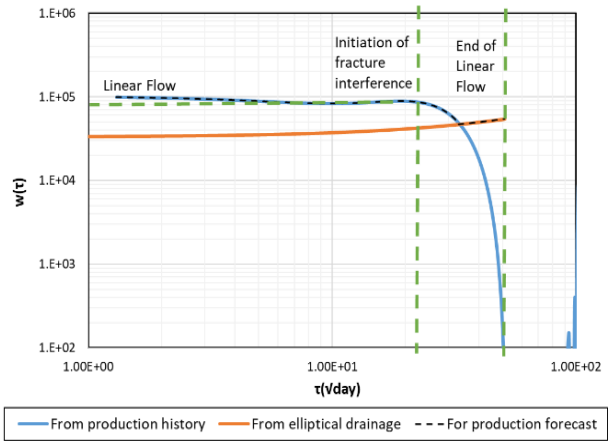

Figure 11: w(τ) plot from production history, elliptical drainage and the values used for forecast (Reprinted with permission from Ankit Bansal and King (2020))

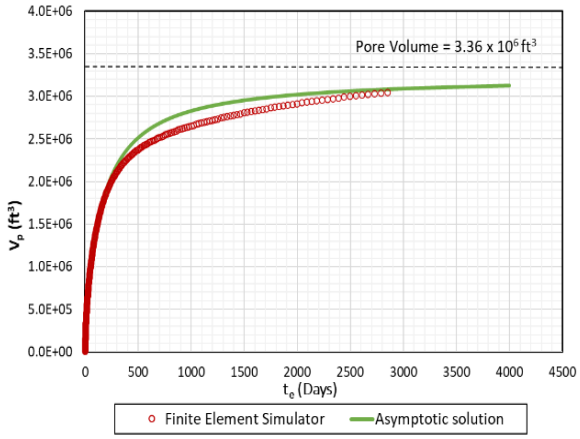

Figure 12: Drainage volume approaches the pore volume (Reprinted with permission from Ankit Bansal and King (2020))

The oil production forecast result are similar to that from the simulator (Figure 13). The contant PI and flowing material balance flow gives us the slope: the x-intercept which is an estimate of ultimate recovery (UR). The estimated reservoir pore volume is 2.40E+05 ft^3 (Figure 14). The estimate is close to the theoretical UR.= $\Delta p_{wf}.c_t.PV$ = 2.52E+05 ft^3.

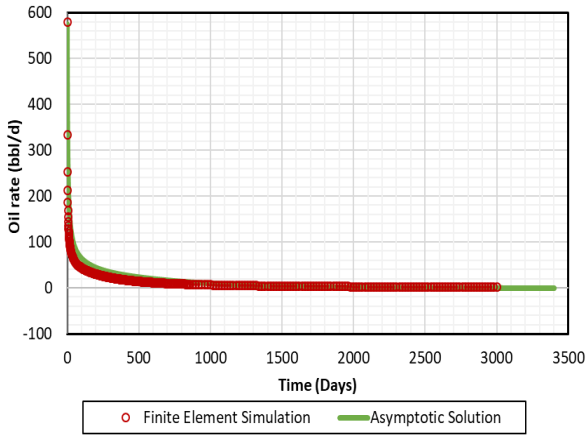

Figure 13 : Oil production rate forecasted matched the historical production from the simulator (Reprinted with permission from Ankit Bansal and King (2020))

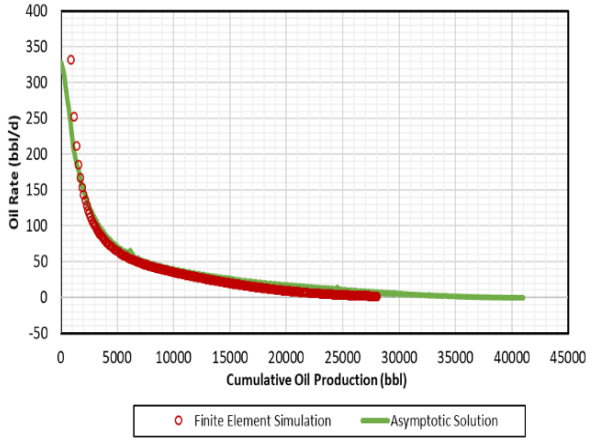

Figure 14 : Flowing material balance approximation provide a reliable estimate of Ultimate Recovery (Reprinted with permission from Ankit Bansal and King (2020))

Field Example

An Eagle ford well with a production history of two years is presented in Figure 15 and Figure 16. The total liquid production is calculated by combining all the phases at reservoir conditions. The BHP is calculated from the frictional and potential head pressure drop. The well produces at a constant BHP of around 3500 psi. Outlier and noise removal techniques were implemented to reduce uncertainities in the results. The well has multiphase flow, however, the fluid is considered slightly compressible because oil is the primary component. The reservoir, well bore and fluid calculations used for the analysis are presented in Table 5**.**

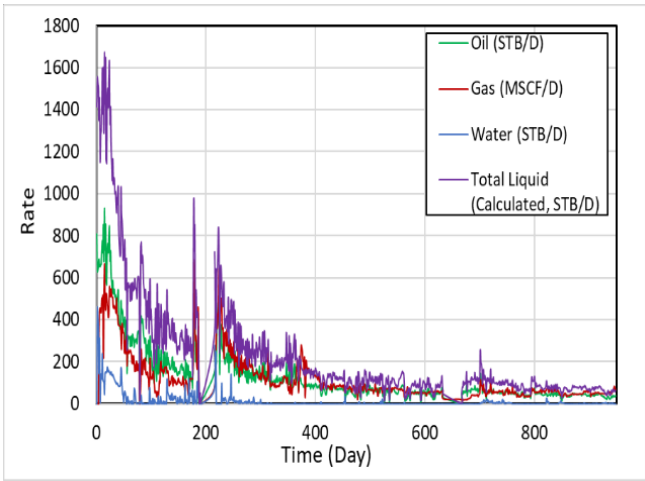

Figure 15: Production profile of Eagle Ford well (Reprinted with permission from Ankit Bansal and King (2020))

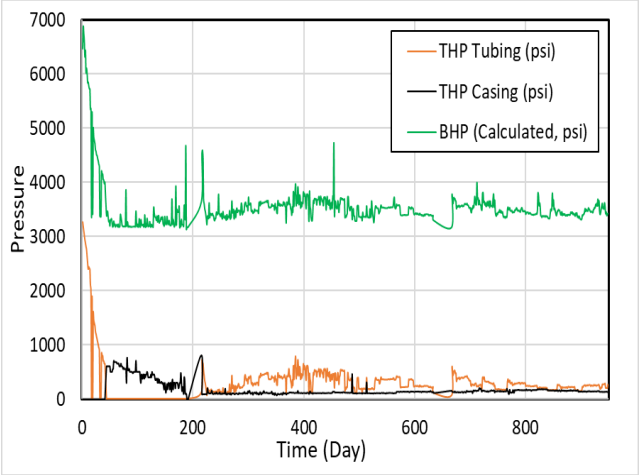

Figure 16: Flowing pressure profile of Eagle Ford well (Reprinted with permission from Ankit Bansal and King (2020))

From Figure 17, we see that the end of linear flow occurs at τ_{ifi}= 45 √day. The calculated reservoir properties are presented in Table 6. The matrix permeability from the asymptotic

solution is around the range of 1.01E-08 to 2.35E-05 mD, as determined from SCAL analysis. Higher fracture area indicates the large number of active fractures created during stimulation.

Table 5: Reservoir, fluid and wellbore properties of the Eagle Ford well (Reprinted with permission from Ankit Bansal and King (2020))

Property	Value	Unit
h	150	ft
n_f	108	
x_s	53	ft
p_i	8125	psi
T_{res}	270	^oF
ϕ	0.082	
L_w	5347	ft
p_{wf}	3700	psi
PV_{res}	8.99E+07	ft^3
c_t	1.2E-05	psi^{-1}
vis	0.327	cp

Table 6: Reservoir parameters derived from the asymptotic solution for the Eagle Ford well (Reprinted with permission from Ankit Bansal and King (2020))

Property	Derived from the Asymptotic Solution	Unit
k_m	3.9669e-05	mD
α	0.7803	ft^2/day
A_f	7.9648e+06	ft^2
x_f	123	ft

In Figure 17, the boundry of the reservoir is determined at τ_e = 668 √days. The w(τ) function is extrapolated based on an elliptical drainage volume and the drainage volume converges to the pore volume (Figure 18).

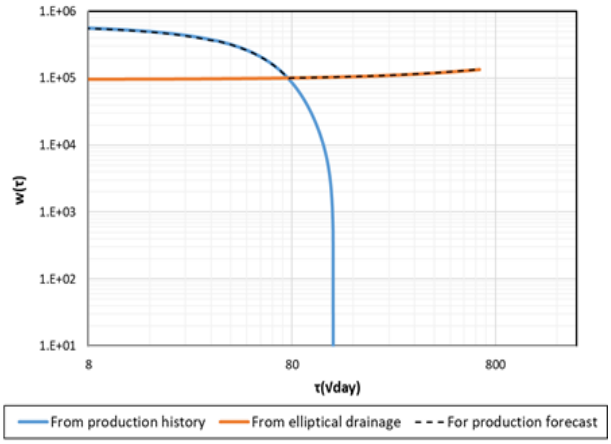

Figure 17: w(τ) plot from production history, elliptical drainage and the values used for forecast (Reprinted with permission from Ankit Bansal and King (2020))

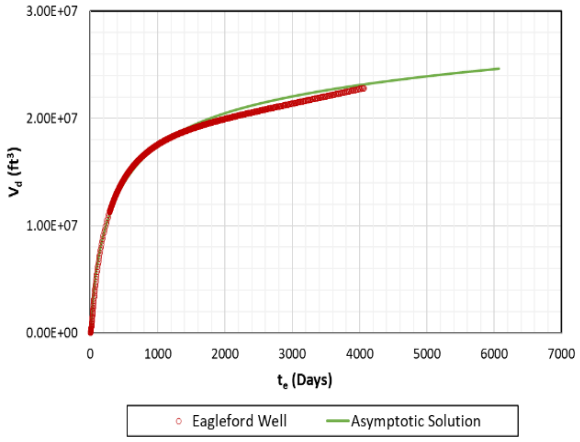

Figure 18: Drainage volume approaches the pore volume for the Eagle Ford well. (Reprinted with permission from Ankit Bansal and King (2020))

Duong Decline curve fit (Duong, 2011) is compared to the results from the asymptotic solution in Figure 19. The Duong decline curve models long transient linear flow regime and provides a higher production rate during the boundary dominated flow. Based on the flowing material balance plot in Figure 20, the Duong decline curve never converges to an UR but the asymptotic solution does gives an UR = 1.46E+07 ft^3.

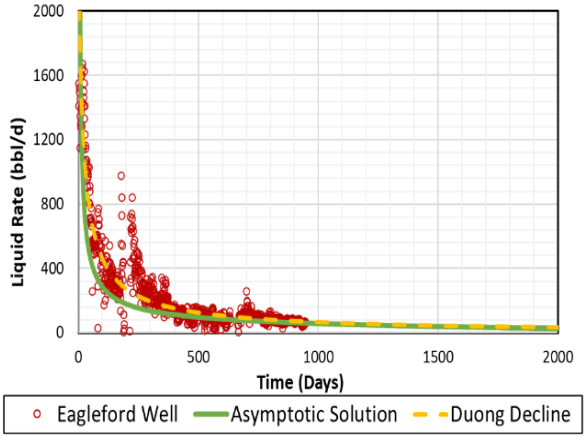

Figure 19: Production forecast and history match for the Eagle Ford well (Reprinted with permission from Ankit Bansal and King (2020))

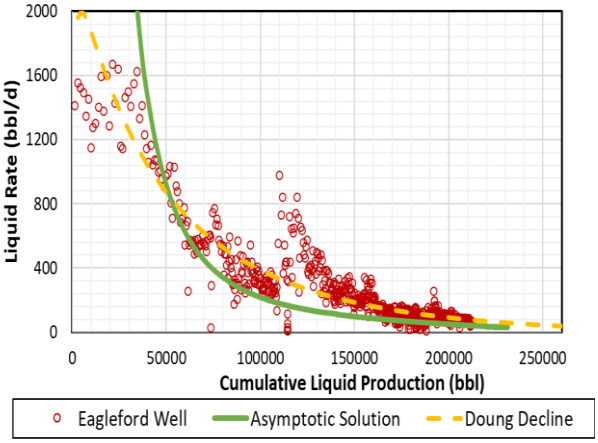

Figure 20: Flowing material balance plot for the Eagle Ford well (Reprinted with permission from Ankit Bansal and King (2020))

Sensitivity Analysis

The input parameters for the asymptotic solution have inherent uncertainties due to the methods used to acquire the data. The bottom hole pressure may be uncertain due to changes in tubular flow regime and a lack of bottom hole sensors. Pore Volume is calculated as $l_w \cdot x_s \cdot h \cdot \phi$ where the fracture spacing may be uncertain because the fractures tend to close over time. The w(τ) plot also provides an diagnostic for partial completion effects (Xue et al., 2019).

Sensitivity plots for changes in the UR and squared residual for the production history decline curve fit are presented in Figure 21 and Figure 22. All parameters were run with a hundred percent variation and the bottom hole flowing pressure has the maximum impact on the decline curve fit. The change in pore volume and fracture spacing do not affect the decline curve fit. Changes in the pore volume significantly impacts the Ultimate recovery. Reducing the pore volume below the 80% of the base case volume produces negative production rate.

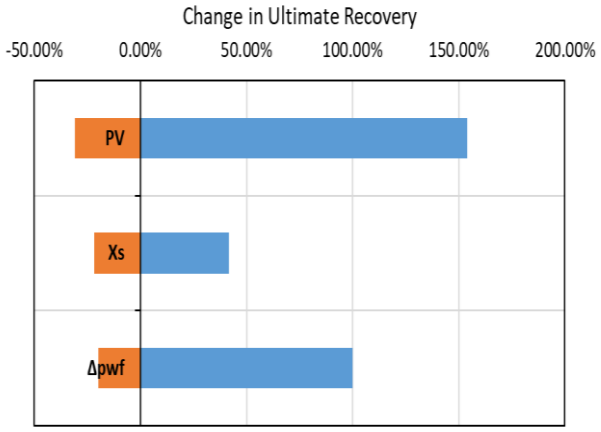

Figure 21: Change in UR due to parameter sensitivity for Eagle Ford well (Reprinted with permission from Ankit Bansal and King (2020))

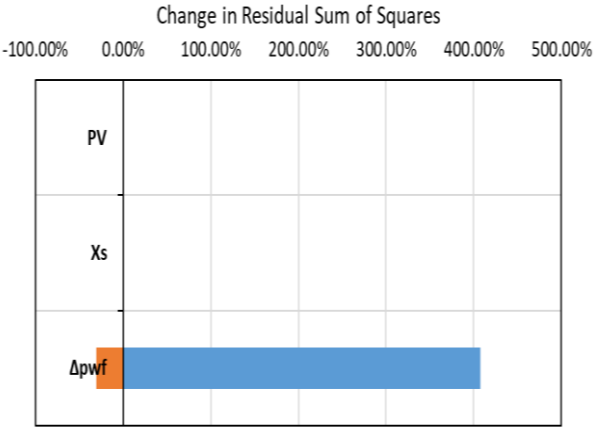

Figure 22: Change in RSS history match due parameter sensitivity for Eagle Ford well (Reprinted with permission from Ankit Bansal and King (2020))

The production forecast was generated for different variations in pore volume and are presented in Figure 23. The flowing material balance forecast leads to variations in the UR from 1.01 to 3.7 MMSCF as presented in Figure 24. Here, we do not present the

uncertainty in Bottom hole flowing pressure because the value is known with high certainty and remains constant over time (Figure 16).

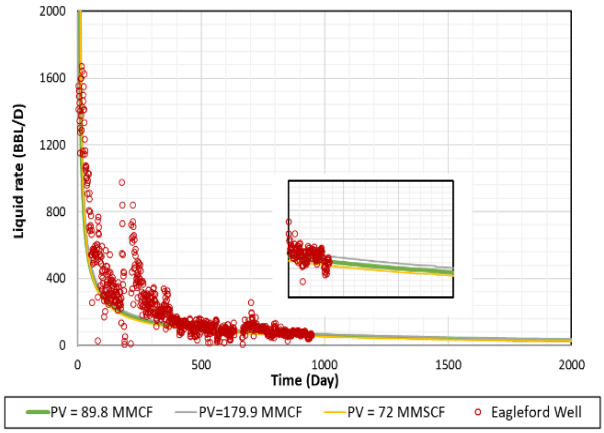

Figure 23: Production forecasts showing the impact of uncertainty in pore volume (Reprinted with permission from Ankit Bansal and King (2020))

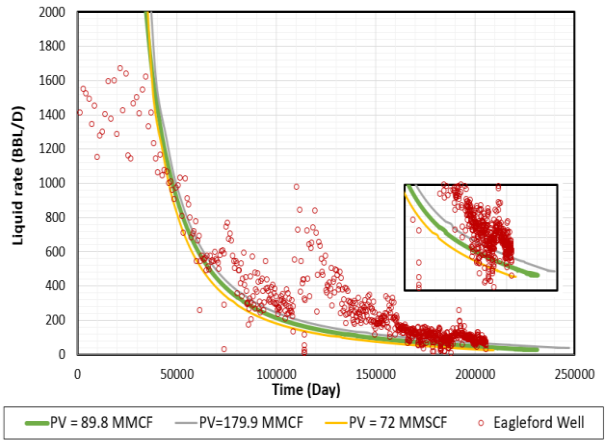

Figure 24: Flowing material balance plot showing the impact of uncertainty in pore volume (Reprinted with permission from Ankit Bansal and King (2020))

CHAPTER IV

CONCLUSIONS AND RECOMMENDATIONS

Conclusion

In this dissertation, we developed an application 'SPADES' to generate novel diagnostic plots based on w(τ) and Drainage volume. These plots help in the identification of characteristic signatures that imply complex fracture geometry, formation linear flow, partial reservoir completions, fracture interference. In the second chapter, we discuss the development of the SPADES application based on an Excel-Python platform. A flowchart explaining the two methods: Outlier Noise removal and the Arp's decline curve fit, is presented. The Outlier and Noise removal algorithms have been explained, and the methods to optimize their tuning parameter is also presented. The AIC-BIC are penalized likelihood criteria used to select the tuning parameter to implement regularized least square optimization for drainage volume inversion. We also discuss the Xlwings plug-in that is used to interface between Python and Excel. The use of Python for back end calculation lets us have access to advanced scientific libraries and Excel in the front end provides the user with a friendly interface.

In the third chapter, we extended the asymptotic solution of the diffusivity equation to production forecasting. The transient solution for no flow boundary is used to model the production behavior of unconventional reservoirs. We explain the workflow to implement this technique: First, we use a data driven drainage volume inversion to model the linear

flow regime, then we determine the reservoir properties and model the boundary dominated flow regime. The concept is first validated using a finite element simulation model. Then we implement the technique for an Eagle Ford well and perform sensitivity analysis based on pore volume, bottom hole pressure and fracture half length. It is seen that bottom hole pressure holds the most significant impact in the production history match. However, unconventional wells can be produced at a constant BHP and have little uncertainty associated with it.

Recommendations

The following points are recommended as an extension/improvement to current dissertation:

1. In the second chapter, for the field application, the drainage volume calculation is based on Outlier and Noise removal which significantly improves the resolution of the reservoir response. We recommend further investigation into field cases that'll provide a strong basis to understanding the various phenomenon occurring in the field and extend the technique beyond its current scope of application.

2. In the third chapter, an application may be developed to implement the production forecasting method. We do not propose this method as a replacement to current decline curve methods, however this method holds significant importance in field level planning and understanding the behavior of type wells.

REFERENCES

Ali, T. A., & Sheng, J. J. (2015). *Production Decline Models: A Comparison Study*. Paper presented at the SPE Eastern Regional Meeting, Morgantown, West Virginia, USA. https://doi.org/10.2118/177300-MS

Ankit Bansal, & King, M. (2020). *Applications of the Diffusive Time of Flight to a Data Driven Approach for Decline Curve Analysis*. Paper presented at the Unconventional Resources Technology Conference Austin, USA.

Arps, J. J. (1945). Analysis of Decline Curves. *Transactions of the AIME, 160*(01), 228-247. doi:10.2118/945228-g

Bourdet, D. (2002). *Well test analysis : the use of advanced interpretation models* (1st ed.). Amsterdam ; Boston: Elsevier.

Chaudhary, N. L., & Lee, W. J. (2016). *Detecting and Removing Outliers in Production Data to Enhance Production Forecasting*. Paper presented at the SPE/IAEE Hydrocarbon Economics and Evaluation Symposium, Houston, Texas, USA. https://doi.org/10.2118/179958-MS

Datta-Gupta, A., Xie, J., Gupta, N., King, M. J., & Lee, W. J. (2011). Radius of Investigation and its Generalization to Unconventional Reservoirs. *Journal of Petroleum Technology, 63*(07), 52-55. doi:10.2118/0711-0052-JPT

Duong, A. N. (2011). Rate-Decline Analysis for Fracture-Dominated Shale Reservoirs. *SPE Reservoir Evaluation & Engineering, 14*(03), 377-387. doi:10.2118/137748-pa

Dziak, J. J., Coffman, D. L., Lanza, S. T., Li, R., & Jermiin, L. S. (2019). Sensitivity and Specificity of Information Criteria. *bioRxiv*, 449751. doi:10.1101/449751

EIA. (2020). Frequently Asked Questions (FAQs) - U.S. Energy Information Administration (EIA). Retrieved from https://www.eia.gov/tools/faqs/faq.php?id=847&t=6

Fetkovich, M. J. (1980). Decline Curve Analysis Using Type Curves. *Journal of Petroleum Technology, 32*(06), 1065-1077. doi:10.2118/4629-pa

Horne, R. N. (1995). *Modern well test analysis : a computer-aided approach* (2nd ed.). Palo Alto, CA: Petroway.

Ilk, D., Jenkins, C. D., & Blasingame, T. A. (2011). *Production Analysis in Unconventional Reservoirs - Diagnostics, Challenges, and Methodologies*. Paper presented at the North American Unconventional Gas Conference and Exhibition, The Woodlands, Texas, USA. https://doi.org/10.2118/144376-MS

Kanfar, M., & Wattenbarger, R. (2012). *Comparison of Empirical Decline Curve Methods for Shale Wells*. Paper presented at the SPE Canadian Unconventional Resources Conference, Calgary, Alberta, Canada. https://doi.org/10.2118/162648-MS

King, M. J., Wang, Z., & Datta-Gupta, A. (2016). *Asymptotic Solutions of the Diffusivity Equation and Their Applications*. Paper presented at the SPE Europec featured at 78th EAGE Conference and Exhibition, Vienna, Austria. https://doi.org/10.2118/180149-MS

Kulkarni, K. N., Datta-Gupta, A., & Vasco, D. W. (2001). A Streamline Approach for Integrating Transient Pressure Data Into High-Resolution Reservoir Models. *SPE Journal, 6*(03), 273-282. doi:10.2118/74135-PA

Lee, J. (1982). *Well testing*. New York: Society of Petroleum Engineers of AIME.

Lee, J., Rollins, J. B., & Spivey, J. P. (2003). *Pressure transient testing*. Richardson, Tex.: Henry L. Doherty Memorial Fund of AIME, Society of Petroleum Engineers.

Lee, W. J., & Sidle, R. (2010). Gas-Reserves Estimation in Resource Plays. *SPE Economics & Management, 2*(02), 86-91. doi:10.2118/130102-pa

Mishra, S. (2014). *Exploring the Diagnostic Capability of RTA Type Curves*. Paper presented at the SPE Annual Technical Conference and Exhibition, Amsterdam, The Netherlands. https://doi.org/10.2118/173481-STU

Novelty and Outlier Detection — scikit-learn 0.23.1 documentation. Retrieved from https://scikit-learn.org/stable/modules/outlier_detection.html

Okouma Mangha, V., Ilk, D., Blasingame, T. A., Symmons, D., & Hosseinpour-zonoozi, N. (2012). *Practical Considerations for Decline Curve Analysis in Unconventional Reservoirs - Application of Recently Developed Rate-Time Relations*. Paper presented at the SPE Hydrocarbon Economics and Evaluation Symposium, Calgary, Alberta, Canada. https://doi.org/10.2118/162910-MS

Sadeghi, M., & Behnia, F. (2018). Optimum window length of Savitzky-Golay filters with arbitrary order. *arXiv preprint arXiv:1808.10489*.

Savitzky, A., & Golay, M. J. E. (1964). Smoothing and Differentiation of Data by Simplified Least Squares Procedures. *Analytical Chemistry, 36*(8), 1627-1639. doi:10.1021/ac60214a047

Song, B., & Ehlig-Economides, C. A. (2011). *Rate-Normalized Pressure Analysis for Determination of Shale Gas Well Performance*. Paper presented at the North American Unconventional Gas Conference and Exhibition, The Woodlands, Texas, USA. https://doi.org/10.2118/144031-MS

Tan, L., Zuo, L., & Wang, B. (2018). Methods of Decline Curve Analysis for Shale Gas Reservoirs. *Energies, 11*, 552. doi:10.3390/en11030552

Thambynayagam, R. K. M. (2011). *The diffusion handbook : applied solutions for engineers*. New York: McGraw-Hill.

Vasco, D. W., & Datta-Gupta, A. (1999). Asymptotic solutions for solute transport: A formalism for tracer tomography. *Water Resources Research, 35*(1), 1-16.

Wang, Z. (2018). *Asymptotic Solutions to the Diffusivity Equation: Validation and Field Applications.* (Ph.D.), Texas A & M University, Retrieved from http : / /hdl .handle .net /1969 .1 /174424.

Wang, Z., Malone, A., & King, M. J. (2019). Quantitative production analysis and EUR prediction from unconventional reservoirs using a data-driven drainage volume formulation. *Computational Geosciences*. doi:10.1007/s10596-019-09833-8

Winestock, A. G., & Colpitts, G. P. (1965). Advances in Estimating Gas Well Deliverability. *Journal of Canadian Petroleum Technology, 4*(03), 111-119. doi:10.2118/65-03-01

Xue, X., Yang, C., Park, J., Sharma, V. K., Datta-Gupta, A., & King, M. J. (2019). Reservoir and Fracture-Flow Characterization Using Novel Diagnostic Plots. *SPE Journal, 24*(03), 1248-1269. doi:10.2118/194017-pa

Yang, C., Sharma, V. K., Datta-Gupta, A., & King, M. J. (2015). *A Novel Approach for Production Transient Analysis of Shale Gas/Oil Reservoirs*. Paper presented at the Unconventional Resources Technology Conference, San Antonio, Texas, USA. https://doi.org/10.15530/URTEC-2015-2176280

Zhang, J., Zou, T., & Tian, C. (2017). Application of Data Smoothing Method in Signal Processing for Vortex Flow Meters. *ITM Web of Conferences, 11*, 01014. doi:10.1051/itmconf/20171101014

Zhang, Y., Bansal, N., Fujita, Y., Datta-gupta, A., King, M. J., & Sankaran, S. (2014). *From Streamlines to Fast Marching: Rapid Simulation and Performance Assessment of Shale Gas Reservoirs Using Diffusive Time of Flight as a Spatial Coordinate*. Paper presented at the SPE Unconventional Resources Conference, The Woodlands, Texas, USA. https://doi.org/10.2118/168997-MS

Zhang, Y., Bansal, N., Fujita, Y., Datta-Gupta, A., King, M. J., & Sankaran, S. (2016). From Streamlines to Fast Marching: Rapid Simulation and Performance Assessment of Shale-Gas Reservoirs by Use of Diffusive Time of Flight as a Spatial Coordinate. *SPE Journal, 21*(05), 1883-1898. doi:10.2118/168997-PA